

# Highly Permeable Polymers of Intrinsic Microporosity (PIM-1)-based Flat Dense and Hollow Fiber Membranes for Gas Separation

Wai Fen Yong<sup>a</sup>, Tai-Shung Chung<sup>a\*</sup>

<sup>a</sup>Department of Chemical & Biomolecular Engineering,  
National University of Singapore, 4 Engineering Drive 4,  
Singapore 117576, Singapore

\*Correspondence author. Tel: +65 6516 6645; fax: +65 67791936.

*E-mail address:* [chencts@nus.edu.sg](mailto:chencts@nus.edu.sg) (T.-S. Chung).

## Abstract

The sky-high crude oil price has diverted the sole demand on it by increasing the use of natural gas and hydrogen for electricity production. However, the prevailing challenge is removing the CO<sub>2</sub> content in these raw gases. Among various separation technologies, polymer-based membrane separation technology have become attractive due to its environmentally benign, small footprint, easy processability and cost competitiveness. In recent years, polymers of intrinsic microporosity, e.g., PIM-1 have emerged as attractive materials for gas separation and energy development because of its high permeability. We report here three approaches in tuning the permeability and selectivity with the incorporation of PIM-1.

In the first and second works, both flat sheet and hollow fiber PIM-1/Matrimid membranes were fabricated. The inclusion of PIM-1 into Matrimid results in a substantial increase in gas permeability and a slight decrease in selectivity. The additions of 5 and 10 wt% PIM-1 into Matrimid induce the permeability increments of 25% and 77%, respectively without compromising its CO<sub>2</sub>/CH<sub>4</sub> selectivity. At binary gas tests of CO<sub>2</sub>/CH<sub>4</sub> (50%/50%), the 30 wt% PIM-1 in Matrimid membrane has a CO<sub>2</sub> permeability of 50 Barrer and a CO<sub>2</sub>/CH<sub>4</sub> selectivity of 31. In addition, the CO<sub>2</sub> permeance of as-spun fibers containing 5 and 10 wt% PIM increases 78% and 146%, respectively without compromising CO<sub>2</sub>/CH<sub>4</sub> selectivity as compared to Matrimid. The CO<sub>2</sub> permeance of the fiber containing 15 wt% PIM-1 displays a greater improvement of 2.8 folds to 243.2 GPU with a CO<sub>2</sub>/CH<sub>4</sub> selectivity of 34.3. Under binary gas tests of 50/50 CO<sub>2</sub>/CH<sub>4</sub>, this fiber shows a CO<sub>2</sub> permeance of 188.9 GPU and a CO<sub>2</sub>/CH<sub>4</sub> selectivity of 28.8. The same fiber also has an impressive O<sub>2</sub> permeance of 3.5 folds higher than the pristine Matrimid with an O<sub>2</sub>/N<sub>2</sub> selectivity of 6.1. The newly developed membranes demonstrate an exceptional gas separation performance and have a great potential to be used for natural gas purification, air separation and CO<sub>2</sub> capture.

The third work reported a simple method to tailor the intrinsic properties of PIM-1 membranes from CO<sub>2</sub>- to H<sub>2</sub>-selective via blending with Matrimid and subsequently cross-linking the membranes by diamines at room temperature. The diamine cross-linking successfully alters the membrane morphology from a dense structure to a composite structure, which consists of a dense layer selective layer at both sides of the outer surface and a porous inner structure. Interestingly, the ideal H<sub>2</sub>/CO<sub>2</sub> selectivity of the membrane after modification by 2 hr triethylenetetramine (TETA) improved dramatically from 0.4-0.8 to 9.6 with a H<sub>2</sub> permeability of 395 Barrer. The modified membranes also show superior separation performance surpassing the present upper bound for H<sub>2</sub>/CO<sub>2</sub>, H<sub>2</sub>/N<sub>2</sub>, H<sub>2</sub>/CH<sub>4</sub> and O<sub>2</sub>/N<sub>2</sub> separations. For a binary H<sub>2</sub>/CO<sub>2</sub> (50%/50%) test, the 2 hr TETA modified membrane shows a H<sub>2</sub> permeability of 205 Barrer and a H<sub>2</sub>/CO<sub>2</sub> selectivity of 5.3. The newly developed TETA modified membrane reveals a competitive alternative for H<sub>2</sub> purification.

**Keywords:** gas separation; membrane separation technology; polyimide; polymer blend

## 1. Introduction

The increase in energy demand has resulted in higher energy prices as well as accelerated the depletion of crude oil in the world. The sky-high crude oil price has diverted the sole demand on it by increasing the use of natural gas for electricity production. The U.S. Energy Information Administration (EIA) estimates that natural gas production will increase from 69.9 Bcf/d in 2013 to 70.4 Bcf/d in 2014 [1]. Natural gas reveals distinct advantages such as stable supply and low energy costs due to its abundant supply. Other than natural gas, hydrogen is revealed as the alternative fuel source. Generally, hydrogen is an environmentally benign energy carrier and an essential feedstock for chemical industry. About 80 % of hydrogen is generated from steam reforming of natural gas [2]. However, the resultant product is contaminated by CO<sub>2</sub>, CH<sub>4</sub>, H<sub>2</sub>O and CO. The prevailing challenge is removing the CO<sub>2</sub> in these raw gases.

The conventional techniques for CO<sub>2</sub> removal are amine absorption, pressure swing adsorption and cryogenic separation which are very energy intensive [3]. Membrane gas separation stands out as a potential technique because of its environmental friendliness, low cost, systemic simplicity and space saving features [3, 4]. Nevertheless, a robust and high performance membrane is desperately required. However, to date, the polymeric membrane in the market suffers from the upper bound trade-off between permeability and selectivity where a high permeability membrane always comes along with a low selectivity and vice versa [5, 6].

In recent years, a novel class of polymers, polymers of intrinsic microporosity (PIMs) has gained much attention due to their large surface area, highly rigid and contorted molecular structure that yield a large fractional free volume (FFV) [7, 8]. Generally, PIMs have a large FFV due to the contorted site groups that kinked the backbone structure with a loose chain packing. In particular, PIMs inherit an effective pore dimension of less than 2 nm which make them behave like molecular sieves. With the existence of microporous structure in PIMs, PIMs membranes show extremely high gas permeability. Besides, PIMs are glassy polymers and amorphous structure in nature and they have high thermal stability. Among all PIMs, the synthesis of PIM-1 has been maturely developed and revalidated by different researchers [7-10].

Taking into account the superior gas permeability of PIM-1, therefore, we incorporated this polymer in three different approaches in order to tune the gas separation properties of membranes. To develop novel separation membranes with enhanced gas separation properties, the scopes of this work are (1) fabrication of dense membranes for CO<sub>2</sub>/CH<sub>4</sub> and O<sub>2</sub>/N<sub>2</sub> separation, (2) production of hollow fiber membranes for CO<sub>2</sub>/CH<sub>4</sub> and O<sub>2</sub>/N<sub>2</sub> separation and (3) development of dense membranes for H<sub>2</sub>/CO<sub>2</sub> separation. It is envisioned that this fundamental study may provide the basic material research for next-generation high performance gas separation membranes.

## 2. Experimental

### 2.1.1 Dense PIM-1/Matrimid membranes

PIM-1/Matrimid dense films were prepared by a solution casting method with a total 2 wt% polymer concentration in DCM. The solution was then filtered by 1 μm PTFE filter and casted onto a leveled silicon wafer at ambient temperature. The polymer films were formed after most of the solvent had evaporated after three days. The resultant films were dried at 120 °C under vacuum for at least 24 h. The thicknesses of the casted films were about 50 ± 5 μm. The rate of pressure increase (dp/dt) at steady state was used to calculate gas permeability as follows:

$$P = \frac{273 \times 10^{10}}{760} \frac{Vl}{AT \left( p_2 \times \frac{76}{14.7} \right)} \left( \frac{dp}{dt} \right) \quad (2)$$

where  $P$  is the gas permeability of a membrane in Barrer (1 Barrer =  $1 \times 10^{-10} \text{ cm}^3$  (STP)  $\text{cm}/\text{cm}^2\text{s.cmHg}$ ),  $V$  is the volume of the downstream chamber ( $\text{cm}^3$ ),  $A$  refers to the effective membrane area ( $\text{cm}^2$ ),  $l$  is the membrane thickness (cm),  $T$  is the operating temperature (K),  $p_2$  is defined as the upstream operating pressure (psia). The permeability tests were repeated at least three times with different membranes and the average deviation obtained was less than 5 %. The ideal selectivity between two different gases in a polymeric membrane is the ratio of the permeability of single gas as described in Eq. (5):

$$\alpha = \frac{P_A}{P_B} \quad (3)$$

### 2.1.2 Hollow fiber spinning, solvent exchange and post-treatment

To facilitate the spinning process, a binary solvent consisting of THF/NMP (50/50 wt%) was employed in this study. PIM-1 and Matrimid were dissolved separately in THF and NMP. The single-layer hollow fiber membranes were fabricated via a dry-jet wet-spinning process. The spinning process was conducted at ambient temperature. After the nascent fibers extruded from the spinneret, they passed through the air-gap region and entered into the coagulant bath filled up with tap water at room temperature and finally wound up on a take-up drum. After spinning, the as-spun fibers were immersed in tap water for 3 days. Subsequently, the hollow fibers were subjected to three consecutive 30-min solvent exchange by circulating in MEOH and then in  $n$ -hexane with the same procedure to allow the removal of residual solvent. Lastly, the fibers were dried in the air at ambient temperature for 24 h before further characterization and permeation tests. 3-4 modules were prepared for each experimental condition. In each module, it consisted of 5–10 fibers with an effective length of around 15 cm per fiber. In the pure gas tests,  $\text{O}_2$ ,  $\text{N}_2$ ,  $\text{CH}_4$  and  $\text{CO}_2$  were tested at 1 atm at room temperature.

The gas permeance was calculated as follows:

$$\frac{P}{L} = \frac{273.15 \times 10^6}{T} \times \frac{Q}{A\Delta P} = \frac{273.15 \times 10^6}{T} \times \frac{Q}{n\pi D l \Delta P} \quad (2)$$

where  $P/L$  is the gas permeance of hollow fiber membranes in GPU (1 GPU =  $1 \times 10^{-6} \text{ cm}^3$  (STP)/ $\text{cm}^2\text{s.cmHg}$ ),  $T$  is the operating temperature (K),  $Q$  is the pure gas flux ( $\text{cm}^3/\text{s}$ ),  $A$  is the total effective area of fibers ( $\text{cm}^2$ ),  $\Delta P$  is the trans-membrane pressure (cmHg),  $n$  is the total number of fibers in one testing module,  $D$  is the outer diameter of fibers (cm) and  $l$  is the effective length of fibers (cm).

### 2.1.3 Diamine Modification

The PIM-1/Matrimid (90:10) dense membranes were modified by immersion into a methanol solution containing 1.65 M diamine for a stipulated period and subsequently washed with fresh methanol for 5 min to remove the residual unreacted diamine. The membranes were then dried under vacuum at 80 °C in order to remove the residual methanol.

### 2.1.4 Characterizations

The UV absorbance spectra of dense membranes were performed using Shimadzu UV-3600 with the range of 200-800 nm. The cross-sectional morphologies were analyzed using field emission scanning electron microscopy (FESEM JEOL JSM-6700LV). The samples were immersed and

fractured in liquid nitrogen. Then, the specimens were adhered on the stub using a double-side conductive carbon tape and dried under vacuum overnight. Before tests, the samples were coated with a platinum layer using a sputtering coater (JEOL LFC-1300).

### 3. Results and Discussion

#### 3.1. Dense membranes for CO<sub>2</sub>/CH<sub>4</sub> and O<sub>2</sub>/N<sub>2</sub> separation

UV absorbance tests were carried out to study the interaction between PIM-1 and Matrimid. The development of CTCs that observed in UV absorbance tests is attributed to the electron transfer interaction between the electron acceptor and the donor [11, 12]. The nitrogen atoms in Matrimid behave as an electron because of their higher electron density than the carbonyl group while the carbonyl group acts as an acceptor [13]. Besides that, the oxygen atoms of the ether groups in PIM-1 may also behave as a donor. The ether groups in PIM-1 are presumably to promote intermolecular charge transfer interactions with the carbonyl groups in Matrimid during polymer blends and cause the changes in the absorption band.

The UV absorbance band of the blend can be predicted based on the additive law as below:

$$\lambda_b = \phi_1 \lambda_1 + \phi_2 \lambda_2 \quad (9)$$

where  $\lambda_b$  is the UV absorbance band of the blend,  $\lambda_1$  and  $\lambda_2$  are the UV absorbance bands of the pristine components 1 and 2, respectively,  $\phi_1$  and  $\phi_2$  are the respective volume fractions of components 1 and 2, respectively. With the addition of PIM-1 into Matrimid, the UV absorbance band exceeds the predicted value based on the additive law (Figure 1). This result confirms the existence of CTC interactions between PIM-1 and Matrimid after blends. The absorption maxima for all the blends show at an average band of 480 nm and suggest they are from the same CTC interactions [14].

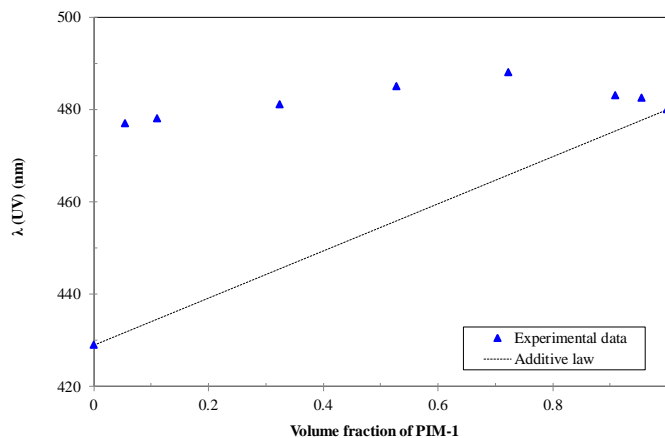


**Figure 1.** UV absorption bands of PIM-1/Matrimid films.

The gas transport properties of the pristine and PIM-1/Matrimid membranes were tested. It can be seen that, on one hand, an increase in PIM-1 content results in an increase in gas permeability of the resultant blends (Figure 2). On the other hand, an increase in PIM-1 content results in a decrease in gas-pair selectivity of the resultant blends. The CO<sub>2</sub> permeability of 5 and 10 wt% of PIM-1 in Matrimid increases from the original 9.6 to 12 and 17 Barrers, respectively, which corresponding to solid increments of 25% and 77% while the CO<sub>2</sub>/CH<sub>4</sub> selectivity drops very slightly (e.g., 2.8% and 5.6%, respectively). The O<sub>2</sub> permeability increases from 2.1 to 2.6 Barrer (e.g., 24% increment) for the PIM-1/Matrimid (5:95) and the O<sub>2</sub>/N<sub>2</sub> selectivity increases

from the original 6.4 to 6.6 (e.g., 3% increment). Compared to Matrimid, the O<sub>2</sub>/N<sub>2</sub> selectivity of the PIM-1/Matrimid (10:90) only has a slight decrease of 5% from 6.4 to 6.1 but its O<sub>2</sub> permeability increases 62% from 2.1 to 3.4 Barrer. Interestingly, there is a peak in the O<sub>2</sub>/N<sub>2</sub> selectivity that exceeding the pristine polymers. It is likely attributed to the formation of charge transfer complexes (CTC) that offering different interaction sites of the functional groups to the O<sub>2</sub> and N<sub>2</sub> gases. Moreover, the enhancement in gas-pair selectivity may due to mild cross-linking in polymer chains results from CTCs. In general, the incorporation of a small loading of PIM-1 in Matrimid not only enhancing the permeability of the Matrimid rich membrane for CO<sub>2</sub>/CH<sub>4</sub> separation without compromising their selectivity, but also remarkably improve their gas transport properties for air separation.

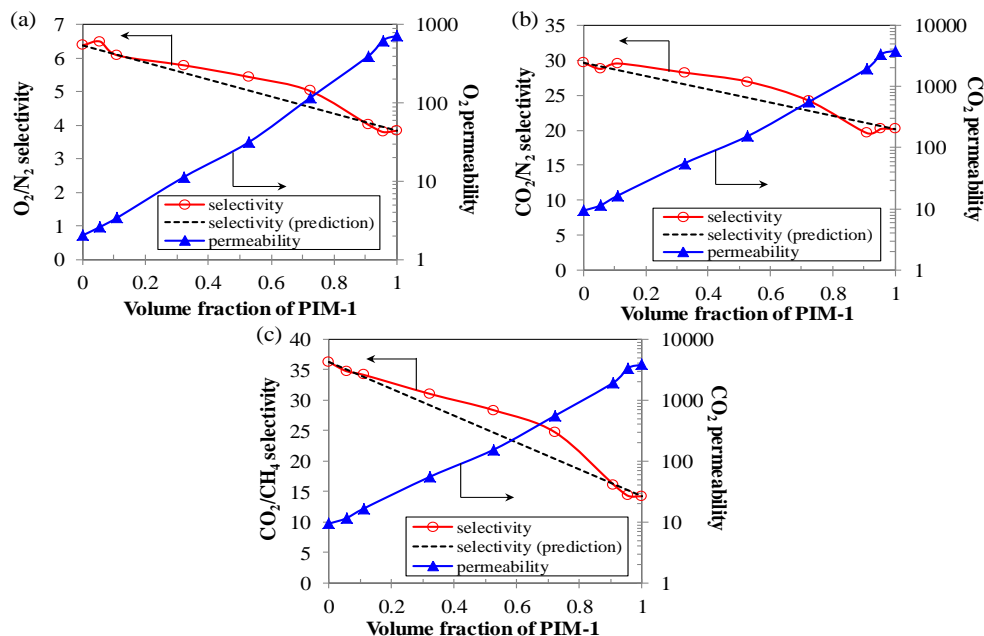


**Figure 2.** Permeability and selectivity of PIM-1/Matrimid membranes.

### 3.2. Hollow fiber membranes for CO<sub>2</sub>/CH<sub>4</sub> and O<sub>2</sub>/N<sub>2</sub> separation

Fibers spun from 5 wt% of PIM-1 in Matrimid show air separation performance as good as defect-free membranes (Figure 3). However, fibers spun from 10 and 15 wt% of PIM-1 in Matrimid show deteriorated gas-pair selectivity comparing to the intrinsic selectivity of dense membranes. This is likely due to the formation of defects at the selective layer with the decrease in compatibility as PIM-1 loading is increased. Besides, different degrees of chain entanglement and molecular chain packing may take place with increasing PIM-1 content [15].

To cure the defects on membrane surface, two post-treatment methods; namely, heat treatment [16-18] and silicon rubber coating [19] have been employed. If there are minor defects on the selective skin of the fibers, they are expected to be easily sealed by heat treatment. The outer surface of the fibers will then be treated with a silicon rubber coating if the defects cannot be mitigated by heat treatment. All fibers reveal remarkable improvements in gas-pair selectivity (Figure 3). Gas permeance increase with an increase in PIM-1 loading and with comparable gas-pair selectivity with the pristine Matrimid membrane. The O<sub>2</sub> and CO<sub>2</sub> permeance of PIM-1/Matrimid (15:85) (condition 3A) hollow fiber membranes after silicon rubber coating is 3.5 folds and 2.8 folds higher, respectively, (e.g., O<sub>2</sub> permeance of 59.9 GPU and CO<sub>2</sub> permeance of 243.2 GPU) with a similar O<sub>2</sub>/N<sub>2</sub> and CO<sub>2</sub>/CH<sub>4</sub> selectivity as compared to the pristine Matrimid.

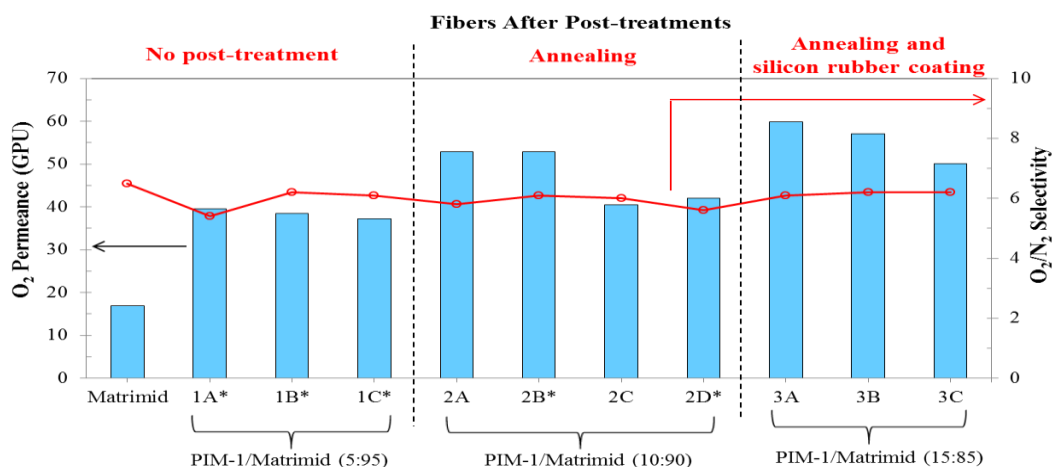


**Figure 3.** A comparison of  $O_2$  permeance and  $O_2/N_2$  selectivity for PIM-1/Matrimid hollow fiber membranes after different post-treatment conditions (\* is the pristine fibers without post-treatment).

The binary gas test consists of  $CO_2/CH_4$  (50%/50%) was conducted for fibers containing 10 and 15 wt% of PIM-1 in Matrimid (Table 1). Compared to the pure gas data, the permeance and selectivity measured under mixed gas tests are slightly lower. The lower in mixed gas permeance of  $CO_2$  and  $CH_4$  is possibly due to the competition effects of two gases in the sorption and transport pathways in the membrane. Thus, the lower in the permeance of the fast gas (e.g.,  $CO_2$ ) results in a decrease in the mixed gas selectivity.

**Table 1.** Binary gas separation performance of PIM-1/Matrimid (15:85) hollow fiber membranes after silicon rubber coating.

Hollow fibers ID	Pure gas <sup>a</sup>			Binary gas <sup>a</sup>		
	Permeance (GPU)		Selectivity	Permeance (GPU)		Selectivity
	$CH_4$	$CO_2$	$CO_2/CH_4$	$CH_4$	$CO_2$	$CO_2/CH_4$
PIM-1/Matrimid (10:90)-2B	8.1	212.4	26.2	6.9	159.7	23.1
PIM-1/Matrimid (15:85)-3A	7.1	243.2	34.3	6.6	188.9	28.8

<sup>a</sup> Pure gas and binary gas conducted at ambient temperature with 1 atm and 2 atm, respectively.

In recent years, polyimide hollow fiber membranes have been studied by various researchers because of its thermal stability and high selectivity [20-32]. The newly developed PIM-1/Matrimid hollow fiber membranes show superior permeance compared to commercial materials [20-32] with a slight decrease in selectivity (Figure 4). The  $O_2$  and  $CO_2$  permeance of the PIM-1/Matrimid hollow fiber membranes are about 3 and 2.5 folds, respectively, higher than the other literature data. This is ascribed to the incorporation of high free volume PIM-1 in Matrimid and the formation of ultra-thin defect-free dense-selective layer hollow fiber membranes. The high performance of PIM-1/Matrimid hollow fiber membranes would definitely enlighten research interest in designing next generation hollow fiber membranes for natural gas separation and air separation.

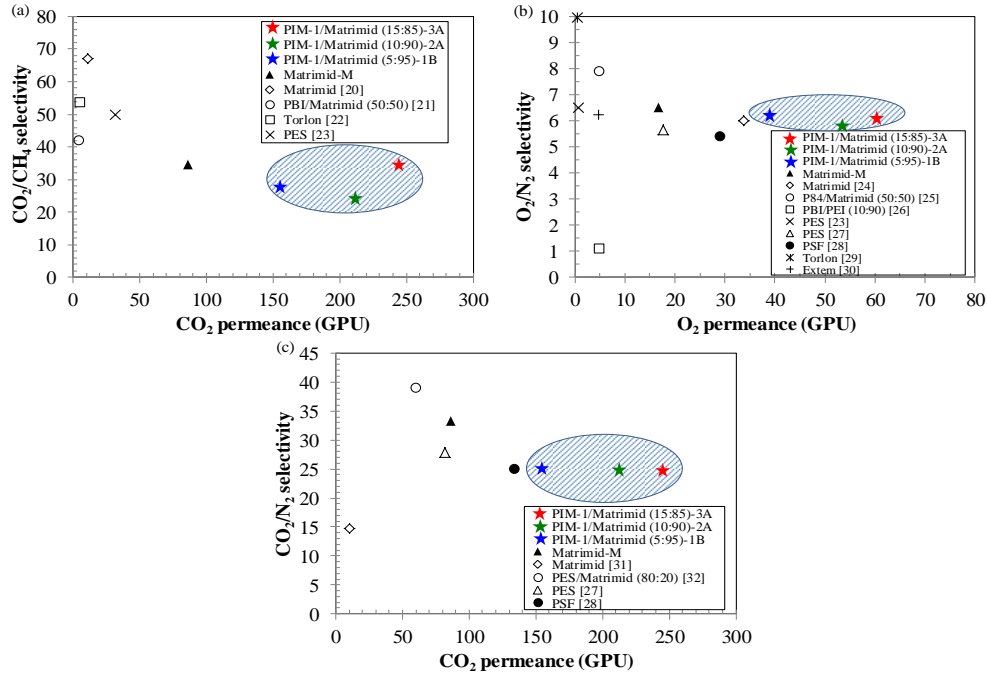


**Figure 4.** A comparison of (a) CO<sub>2</sub>/CH<sub>4</sub>; (b) O<sub>2</sub>/N<sub>2</sub> and (c) CO<sub>2</sub>/N<sub>2</sub> separation performance of PIM-1/Matrimid membranes with other commercial materials.

### 3.3. Dense membranes for H<sub>2</sub>/CO<sub>2</sub> separation

To develop membranes with superior performance for H<sub>2</sub> purification, PIM-1 was employed as a base membrane material in this study. PIM-1 was blended with a small loading of Matrimid and then modified by diamine cross-linking. The cross-sectional morphologies of the membranes before and after 1 hr and 2 hr TETA modifications were examined (Figure 5). The pristine PIM-1/Matrimid (90:10) membrane shows a fully dense structure. After triethylenetetramine (TETA) modification, the membrane exhibits a porous middle bulk structure and a very thin dense selective-layer at the outer surface which is less than 100 nm. The porous structure at the middle bulk is attributed to the methanol-induced swelling while the very thin dense selective-layer is formed by the TETA cross-linking reaction.

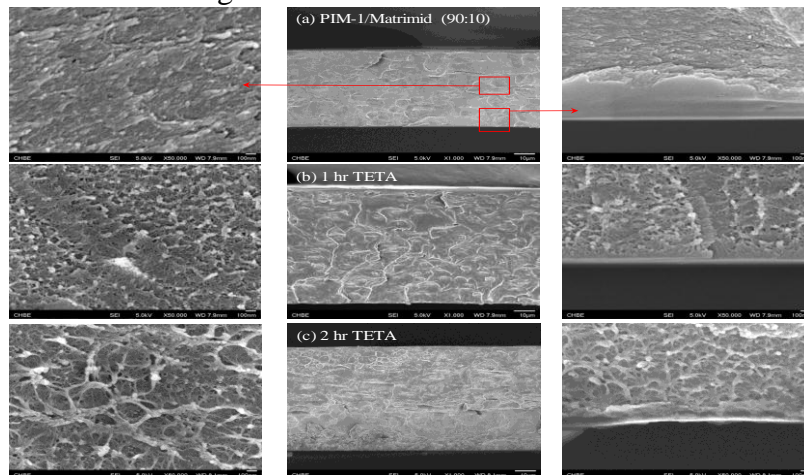


**Figure 5.** FESEM cross-sectional morphologies of (a) the pristine PIM-1/Matrimid (90:10); (b) 1 hr TETA and (c) 2 hr TETA modified membranes.

For the binary  $H_2/CO_2$  (50%/50%) test, the 2 hr TETA modified membrane has a  $H_2$  permeability of 205 Barrer and a  $H_2/CO_2$  selectivity of 5.3 (Table 2). The slight decrease in  $H_2$  permeability and  $H_2/CO_2$  selectivity in binary gas tests are ascribed to the sorption competition between  $H_2$  and  $CO_2$ . The gas separation performance of the TETA cross-linked membranes for all the gas pairs is surpassing the upper bound of the current membranes (Figure 6). The TETA cross-linked membranes show an improvement enhancement with a higher  $H_2$  permeability. The high separation performance of the TETA modified membranes reveals their potential in a highly competitive market for hydrogen purification.

**Table 2.** Binary gas permeability and selectivity of the pristine and TETA modified membranes tested with a  $H_2/CO_2$  (50:50 mole %) at 35 °C and 7 atm.

Membranes ID	Permeability (Barrer) <sup>a</sup>		Selectivity
	$H_2$	$CO_2$	$H_2/CO_2$
PIM-1	603 (2918) <sup>a</sup>	3065 (3825)	0.2 (0.6)
PIM-1/Matrimid (90:10)	907 (2118)	2083 (2855)	0.4 (0.7)
1 hr TETA	166 (463)	44 (72)	3.8 (6.4)
2 hr TETA	205 (395)	38 (41)	5.3 (9.6)

<sup>a</sup> Number in parentheses is the permeability and ideal selectivity obtained from pure gas test.

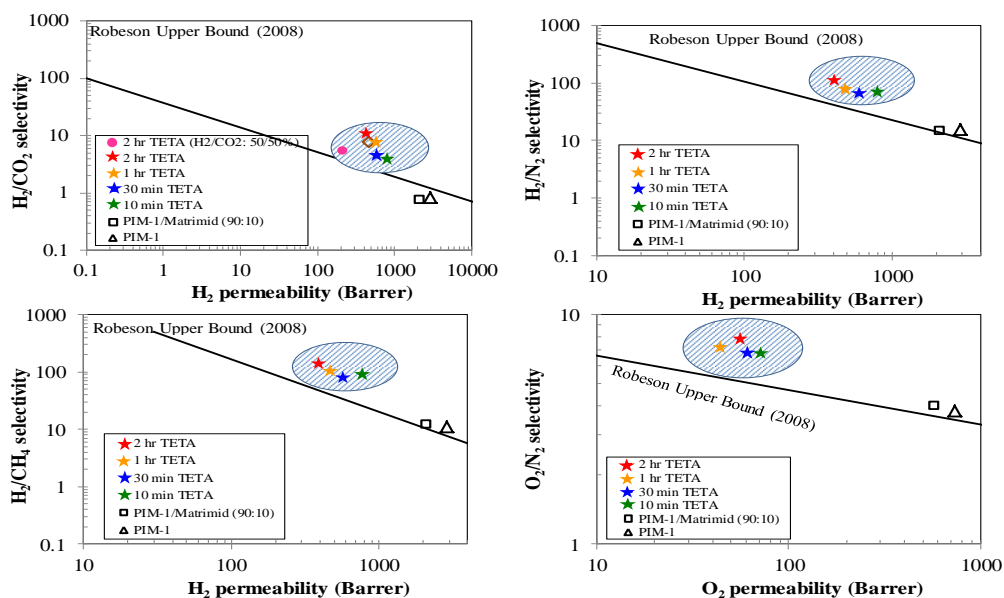


**Figure 6.** A comparison of  $H_2/CO_2$ ,  $H_2/N_2$ ,  $H_2/CH_4$  and  $O_2/N_2$  separation performance of the pristine PIM-1, PIM-1/Matrimid (90:10) and TETA modified membranes with the Robeson upper bound.

#### 4. Conclusions

We have developed high performance PIM-1 based flat sheet and hollow fiber membranes for gas separation, specifically for natural gas, oxygen and hydrogen purification. We have compared the separation performance with literature data and our membranes show an outstanding performance overtakes the existing membranes. The interaction between these PIM-1 and Matrimid is due to the formation of charge transfer complexes. The intrinsic property of PIM-1/Matrimid membrane after diamine cross-linking has tuned from CO<sub>2</sub>- to H<sub>2</sub>-selective which is suitable for hydrogen enrichment processes. Future work is planned to study the long term stability of these newly developed membranes.

#### Acknowledgements

This research is supported by the National Research Foundation, Prime Minister's Office, Singapore under its Competitive Research Program (CRP Award No. NRF-CRP 5-2009-5 (NUS grant number R-279-000-311-281)).

#### References

- [1] Short-Term Energy Outlook, U.S. Energy Information Administration, September 2013.
- [2] T.M. Nenoff, R.J. Spontak, C.M. Aberg, Membranes for hydrogen purification: an important step toward a hydrogen-based economy, *MRS Bull* 31 (2006) 735–744.
- [3] D.R. Paul, Y.P. Yampol'skii, *Polymeric gas separation membranes*, CRC Press, Boca Raton, FL, 1994.
- [4] P. Bernardo, E. Drioli, G. G., Membrane gas separation: A review/state of the art, *Ind. Eng. Chem. Res.*, 48 (2009) 4638–4663.
- [5] A.A. Olajire, CO<sub>2</sub> capture and separation technologies for end-of-pipe applications – A review, *Energy*, 35 (2010) 2610–2628.
- [6] L.M. Robeson, The upper bound revisited, *J. Membr. Sci.* 320 (2008) 390–400.
- [7] P.M. Budd, E.S. Elabas, B.S. Ghanem, S. Makhseed, N.B. McKeown, K.J. Msayib, C.E. Tattershall, D. Wang, Solution-processed, organophilic membrane derived from a polymer of intrinsic microporosity, *Adv. Mater.* 16 (2004) 456–459.
- [8] P.M. Budd, B.S. Ghanem, S. Makhseed, N.B. McKeown, K.J. Msayib, C.E. Tattershall, Polymers of intrinsic microporosity (PIMs): robust, solution-processable, organic nanoporous materials, *Chem. Commun.* (2004) 230–231.
- [9] N. Du, H.B. Park, G.P. Robertson, M.M. Dal-Cin, T. Visser, L. Scoles, M.D. Guiver, Polymer nanosieve membranes for CO<sub>2</sub>-capture applications, *Nat. Mater.* 10 (2011) 372–375.
- [10] J. Song, N. Du, Y. Dai, G.P. Robertson, M.D. Guiver, S. Thomas, I. Pinnau, Linear high molecular weight ladder polymers by optimized polycondensation of tetrahydroxytetramethylspirobisindane and 1,4-dicyanotetrafluorobenzene, *Macromolecules* 41 (2008) 7411–7417.
- [11] M. Hasegawa, M. Kochi, I. Mita, R. Yokota, Molecular aggregation and fluorescence spectra of aromatic polyimides, *Eur. Polym. J.* 25 (1989) 349–354.
- [12] Y.C. Xiao, L. Shao, T.S. Chung, D.A. Schiraldi, Effects of thermal treatments and dendrimers chemical structures on the properties of highly surface cross-linked polyimide films, *Ind. Eng. Chem. Res.* 44 (2005) 3059–3067.
- [13] M. Hasegawa, K. Horie, Photophysics, photochemistry and optical properties of polyimides, *Prog. Polym. Sci.* 26 (2001) 259–335.

- [14] M. Hasegawa, I. Mita, M. Kochi, R. Yokota, Miscibility of polyimide/polyimide blends and charge-transfer fluorescence spectra, *Polymer* 32 (1991) 3225–3232.
- [15] M.M. Teoh, T.S. Chung, K.Y. Wang, M.D. Guiver, Exploring Torlon/P84 co-polyamide-imide blended hollow fibers and their chemical cross-linking modifications for pervaporation dehydration of isopropanol, *J. Membr. Sci.* 61 (2008) 404–413.
- [16] A.Z. Gollan, Anisotropic membranes for gas separation, US Patent 4,681,605 (1987).
- [17] B. Bikson, J.K. Nelson, Composite membranes and their manufacture and use, US Patent 4,826,599 (1989).
- [18] Y. Li, C. Cao, T.S. Chung, K.P. Pramoda, Fabrication of dual-layer polyethersulfone (PES) hollow fiber membranes with an ultrathin dense-selective layer for gas separation, *J. Membr. Sci.* 245 (2004) 53–60.
- [19] J.M.S. Henis, M.K. Tripodi, Composite hollow fiber membranes for gas separation: the resistance model approach, *J. Membr. Sci.* 8 (1981) 233–246.
- [20] G. Dong, H. Li, V. Chen, Factors affect defect-free Matrimid<sup>®</sup> hollow fiber gas separation performance in natural gas purification, *J. Membr. Sci.* 353 (2010) 17–27.
- [21] S.S. Hosseini, N. Peng, T.S. Chung, Gas separation membranes developed through integration of polymer blending and dual-layer hollow fiber spinning process for hydrogen and natural gas enrichments, *J. Membr. Sci.* 349 (2010) 156–166.
- [22] N. Peng, T.S. Chung, J.Y. Lai, The rheology of Torlon<sup>®</sup> solutions and its role in the formation of ultra-thin defect-free Torlon<sup>®</sup> hollow fiber membranes for gas separation, *J. Membr. Sci.* 326 (2009) 608–617.
- [23] Y. Li, T.S. Chung, Y.C. Xiao, Superior gas separation performance of dual-layer hollow fiber membranes with an ultrathin dense-selective layer, *J. Membr. Sci.* 325 (2008) 23–27.
- [24] D.T. Clausi, W.J. Koros, Formation of defect-free polyimide hollow fiber membranes for gas separations, *J. Membr. Sci.* 167 (2000) 79–89.
- [25] T. Visser, N. Masetto, M. Wessling, Materials dependence of mixed gas plasticization behavior in asymmetric membranes, *J. Membr. Sci.* 306 (2007) 16–28.
- [26] T.S. Chung, Z.L. Xu, Asymmetric hollow fiber membranes prepared from miscible polybenzimidazole and polyetherimide blends, *J. Membr. Sci.* 147 (1998) 35–47.
- [27] D.L. Wang, K. Li, W.K. Teo, Highly permeable polyethersulfone hollow fiber gas separation membranes prepared using water as non-solvent additive, *J. Membr. Sci.* 176 (2000) 147–158.
- [28] D.L. Wang, W.K. Teo, K. Li, Preparation and characterization of high-flux polysulfone hollow fibre gas separation membranes, *J. Membr. Sci.* 204 (2002) 247–256.
- [29] N. Peng, T.S. Chung, K.Y. Li, The role of additives on dope rheology and membrane formation of defect-free Torlon<sup>®</sup> hollow fibers for gas separation, *J. Membr. Sci.* 343 (2009) 62–72.
- [30] N. Peng, T.S. Chung, M.L. Chng, W.Q. Aw, Evolution of ultra-thin dense-selective layer from single-layer to dual-layer hollow fibers using novel Extem<sup>®</sup> polyetherimide for gas separation, *J. Membr. Sci.* 360 (2010) 48–57.
- [31] O.C. David, D. Gorri, K. Nijmeijer, I. Ortiz, A. Urriaga, Hydrogen separation from multicomponent gas mixtures containing CO, N<sub>2</sub> and CO<sub>2</sub> using Matrimid<sup>®</sup> asymmetric hollow fiber membranes, *J. Membr. Sci.* 419–420 (2012) 49–56.
- [32] G.C. Kapantaidakis, G.H. Koops, High flux polyethersulfone–polyimide blend hollow fiber membranes for gas separation, *J. Membr. Sci.* 204 (2002) 153–171.